NIH Public Access
Author Manuscript
Cancer Res. Author manuscript; available in PMC 2010 December 15.

Published in final edited form as:
Cancer Res. 2009 December 15; 69(24): 9291–9300. doi:10.1158/0008-5472.CAN-09-2418.

Impaired skin and mammary gland development and increased γ-irradiation-induced tumorigenesis in mice carrying a mutation of S1152-ATM phosphorylation site in Brca1

Sang Soo Kim[1,2,*,a], **Liu Cao**[2,a], **Hye Jung Baek**[1,a], **Sung-Chul Lim**[3], **Cuiling Li**[2], **Rui-Hong Wang**[2], **Xiaoling Xu**[2], **Kwan Ho Cho**[1], and **Chu-Xia Deng**[2,*]

[1] Radiation Medicine Branch, National Cancer Center, Goyang, 410-769, Korea

[2] Genetics of Development and Disease Branch, National Institute of Diabetes, Digestive and Kidney Diseases, National Institutes of Health, 10/9N105, 10 Center Drive, Bethesda, MD 20892, USA

[3] Department of Pathology, College of Medicine, Chosun University, Gwangju, 501-759, Korea

Abstract

The tumor suppressor BRCA1 interacts with many proteins, and undergoes multiple modifications upon DNA damage. ATM, a key molecule of the DNA damage response, phosphorylates S1189 of BRCA1 after γ-irradiation. S1189 of BRCA1 is known as a unique ATM phosphorylation site in BRCA1 exon 11. To study the functions of ATM-dependent phosphorylation of BRCA1-S1189, we generated a mouse model carrying a mutation of S1152A (S1152 in mouse Brca1 corresponds to S1189 in human BRCA1) by gene targeting. *Brca1*$^{S1152A/S1152A}$ mice were born at the expected ratio, unlike that seen in previous studies of Brca1-null mice. However, 36% of *Brca1*$^{S1152A/S1152A}$ mice exhibited aging-like phenotypes including growth retardation, skin abnormalities, delay of the mammary gland morphogenesis with an increase in apoptosis. Mutant mice were hypersensitive to high dose of γ-irradiation, displaying shortening of the lifespan and reduction in intestinal villi size, associated with increased apoptosis. Aging-unaffected 18 month-old *Brca1*$^{S1152A/S1152A}$ female mice also showed mammary gland abnormalities with increased level of cyclin D1, and phospho-ER-α such as Brca1-Δ11 mutation. Upon low dose γ-irradiation, they suffered a marked increase in tumor formation with an abnormal coat pattern. Furthermore *Brca1*$^{S1152A/S1152A}$ embryonic fibroblasts failed to accumulate p53 upon γ-irradiation with delayed phosphorylation of p53-S23. These observations indicate that ATM-mediated phosphorylation of S1189 is required for BRCA1 functions to modulate DNA damage response and suppress tumor formation by regulation of p53 and apoptosis.

Keywords

BRCA1; ATM; longevity; irradiation; tumorigenesis

INTRODUCTION

Ataxia-telangiectasia (A-T) is a human autosomal recessive disorder characterized by progressive neurodegeneration, immunodeficiency, and cancer predisposition (1). The A-T

*Address correspondence to: Sang Soo Kim, Phone: (8231) 920-2491, Fax: (8231) 920-2494, sangsookim@ncc.re.kr, Chu-Xia Deng, Phone: (301) 402-7225, Fax: (301) 480-1135, ChuxiaD@BDG10.NIDDK.NIH.Gov.
[a]These authors contribute equally.

CONFLICT OF INTEREST
The authors declare no conflict of interest.

NIH-PA Author Manuscript
NIH-PA Author Manuscript
NIH-PA Author Manuscript

NIH-PA Author Manuscript

NIH-PA Author Manuscript

NIH-PA Author Manuscript

cellular phenotype includes chromosomal instability, radiosensitivity, and failure to adequately activate cell cycle checkpoints (2). Ataxia-telangiectasia-mutated (ATM), the gene product defective in A-T, is a member of the phosphoinositide 3-kinase (P13-kinase) family, which is involved in the recognition of damage in DNA (3).

Germline mutations in BRCA1 and BRCA2 are responsible for the majority of hereditary breast cancers and cause almost all familial cases involving both breast and ovarian cancers (4,5). The BRCA1protein is a tumor suppressor that has a crucial role in maintenance of genomic integrity. BRCA1 achieves this by integrating important cellular processes, such as regulation of genetic stability, DNA damage repair, centrosome duplication, apoptosis, and cell cycle control (6). *BRCA1* contains24 exons that encode proteins of 1,863 and 1,812 amino acids in the human and mouse, respectively (7,8). Notably, more than 60% of the protein is encoded by an unusually large exon, exon 11, which is 3.4 kb in length. In addition to the full-lengthBRCA1 protein (BRCA1-FL), a deletant, BRCA1-Δ11, arises from in-frame splicing between exon 10 and exon 12, but retains the highly conserved amino-terminal RING finger and carboxyl-terminal BRCT domains found in full-length BRCA1 (9–12). To study the functions of BRCA1 and to create animal models for BRCA1-associated breast cancer, mice carrying various mutations in Brca1 have been generated by gene targeting (reviewed in (13)). Brca1-null embryos die at embryonic (E) day 6.5–8.5 (14–16), whereas embryos that lack Brca1-FL due to targeted deletion of exon-11 ($Brca1^{\Delta 11/\Delta 11}$) but still express the Brca1-Δ11 isoform, die at E 12–18.5 (17). In addition, surviving $Brca1^{\Delta 11/\Delta 11}$ mice that had lost one or both *p53* alleles exhibited aging phenotypes with tumor formation (17,18). Moreover, Cre-mediated excision of exon 11 of *Brca1* in mouse mammary epithelial cells caused abnormal ductal development attributable to induction of apoptosis (19). However, $Brca1^{FL/FL}$ mutant mice which lack Brca1-Δ11 isoform did not display any developmental defects and the incidence of tumor formation in such animals was significantly lower than in $Brca1^{\Delta 11/\Delta 11}$ mice, indicating that exon 11 of Brca1 is essential for proper functioning of Brca1 in development and tumor suppression (20).

The DNA damage response involves the sensing of DNA damage followed by transduction of the damage signal to a network of cellular pathways, including cell cycle checkpoints, DNA repair, and the apoptotic system (21). It has been shown that BRCA1 undergoes regulation by phosphorylation upon DNA damage and cell cycle progression (22). In this network, ATM is also a critical regulator of checkpoint signal cascades, which phosphorylates and activates several molecules including H2AX, p53, and CHK1, to execute the DNA damage response (2,23). ATM also phosphorylates BRCA1 in response to ionizing radiation *in vivo* and *in vitro*, in a region that contains clusters of serine and glutamine residues (24). Analysis by mass spectrometry demonstrated that seven serine residues (S1189, S1330, S1423, S1457, S1466, S1524, and S1542) of BRCA1 were phosphorylated. ATM has also been reported to interact with BRCA1 as part of a large multi-subunit protein complex of tumor suppressors, termed BASC (25). These results indicate that communication between BRCA1 and ATM is critical for an appropriate response to DNA damage and may provide a molecular explanation for the role of BRCA1 and ATM in preventing tumor formation.

However, the functional role of phosphorylation by ATM of BRCA1 in progression of breast cancer remains elusive. To address the potential function of BRCA1 exon 11, we mutated S1152 of mouse Brca1, which equivalents to S1189 of human BRCA1, a unique ATM phosphorylation site in exon 11, and studied the biological consequences using mutant mice and cultured mutant cells. Our data indicate that ATM-mediated phosphorylation of S1152 mediates some Brca1 functions in modulation of homeostasis, longevity, and genetic integrity, and that disruption of this site results in increased tumor formation after DNA damage in mutant mice.

NIH-PA Author Manuscript

NIH-PA Author Manuscript

NIH-PA Author Manuscript

MATERIALS AND METHODS

Mouse treatment and analysis

Mice were monitored at least twice a week for possible symptoms related to illness and tumor formation. Animals were also subjected to γ-irradiation to check sensitivity toward tumorigenesis after DNA damage. In the high dose γ-irradiation study, mice were given a single irradiation of 8 Gy at 8 weeks of age. For the low dose γ-irradiation study, female mice at 8 weeks of age were irradiated with 3 Gy four times at 1 week intervals (26). When mice developed symptoms and tumors, tissues were collected, divided, frozen in liquid nitrogen, and stored at −80°C or fixed in 10% (v/v) buffered formalin and embedded in paraffin for staining. We also carried out whole-mount staining of mammary glands, as previously described (19).

MEF cells and analysis

MEF cells were derived from E14.5 embryos generated from intercrosses of *Brca1*$^{+/S1152A}$ animals. Every comparison was made between wild-type and mutant in same littermates. Analyses of cell cycle arrest were performed as described previously (26). Western blot analysis was performed according to standard procedures using ECL detection (GE Healthcare, Pittsburgh, PA). The following primary antibodies were used: anti-p53 (Millipore, Billerica, MA), anti-p53^{S20} (Cell Signaling, Danvers, MA), and anti-β-actin (Sigma, St. Louis, MO). Horseradish peroxidase-conjugated donkey anti-rabbit or sheep anti-mouse antibodies (GE Healthcare, Pittsburgh, PA) were used as secondary antibodies.

Histology and immunohistochemical staining

For histology, tissues were fixed in 10% (v/v) formalin, embedded in paraffin wax, sectioned, stained with hematoxylin and eosin (H&E), and examined by light microscopy. Detection of antigenic proteins was achieved using the ZYMED histostaining kit (Invitogen, Carlsbad, CA), according to the manufacturer's instructions. The following primary antibodies were used: anti-cyclin D1, anti-phospho-ER-α^{S118} (Cell Signaling), anti-ER-α (Santa Cruz, Santa Cruz, CA), anti-p53 (Novocastra, Newcastle, UK), anti-Ki-67 (Novus, Littleton, CO), anti-K6 (Covance, Princeton, NJ), and anti-AE13 (Abcam, Cambridge, UK). The terminal deoxynucleotidyltransferase-mediated dUTP-biotin nick-end labeling (TUNEL) assay of apoptotic cells and assessment of proliferating cells in tissue sections by BrdU incorporation were performed according to the manufacturers' recommendations (Millipore and Invitogen, respectively).

Statistical analysis

Student's t-test (http://www.physics.csbsju.edu/stats/t-test.html) was used to compare differences in body weight, skin thickness, TUNEL- and BrdU-positive cell numbers, and irradiation-induced survival responses, between *Brca1-S1152A* mutant and control mice, as specified below.

RESULTS

Targeted disruption of the ATM phosphorylation site, S1152, in mouse Brca1

In response to ionizing radiation, ATM phosphorylates BRCA1 at seven serine residues (S1189, S1330, S1423, S1457, S1466, S1524, and S1542) (24). Among these, S1189 is the sole residue conserved in mouse Brca1 and is located in exon11. Thus, we substituted S1152 of mouse Brca1 with A1152, using a co-transfer-type targeting construct (Supplementary Fig. S1A). Southern blot analysis detected homologous recombination at the *Brca1* locus in 10 of 82 G418/FIAU doubly resistant ES clones (Supplementary Fig. S1B and S1C). After

NIH-PA Author Manuscript

NIH-PA Author Manuscript

NIH-PA Author Manuscript

confirming that the mutant cells contained the S1152A mutation by *Apa*I digestion and sequencing (data not shown), three correctly targeted ES clones were injected into blastocysts and germline transmission was obtained from all three. Mice carrying the targeted disruption were further crossed with *EIIa-Cre* transgenic mice that express Cre in the germline (27) to delete the *ploxPneo* gene (Supplementary Fig. S1A). Mice carrying a heterozygous mutation of *Brca1*-S1152A ($Brca1^{+/S1152A}$) were phenotypically normal and were further crossed to produce $Brca1^{S1152A/S1152A}$ animals (Supplementary Fig. S1D). Our data indicated that $Brca1^{S1152A/S1152A}$ mice were present in a Mendelian ratio at weaning (data not shown). Western blot analysis indicated that Brca1-S1152A was expressed in mutant cells at levels similar to those of wild-type protein (Supplementary Fig. S1E). Our analysis indicated that both male and female mice with homozygous mutations of Brca1-S1152A showed no fertility abnormality. This observation indicated that the Brca1-S1152A mutation caused no obvious developmental defects.

$Brca1^{S1152A/S1152A}$ mice exhibit aging-like phenotypes

The $Brca1^{S1152A/S1152A}$ mutant mice survived to adulthood, enabling us to investigate the effect of ATM phosphorylation of Brca1 exon 11 by monitoring phenotypes. We followed a group of mutant mice (n=78) and found that 30 displayed abnormalities within the first year of life (Fig. 1A). Twenty-eight of 30 mice were small, thin, and hyperactive, with severe dermatitis (arrow in Fig. 1A) in the dorsal region, from neck to tail. Two mice died of thymic lymphoma. Simultaneously, we compared the weight of $Brca1^{S1152A/S1152A}$ mice and wild-type animals at 1 month intervals, from 2 months to 11 months (Fig. 1B). The weight of $Brca1^{S1152A/S1152A}$ mice (n=15) did not increase after 6 months and the differences between wild-type and mutant animals were statistically significant after month 7 ($P<0.01$).

To further examine whether the dermatitis resulted from a defect in wound healing, we investigated the healing pattern after skin incision in $Brca1^{S1152A/S1152A}$ mice, compared with wild-type animals. As shown in Fig. 1C, wounded mutant skins healed but displayed either complete failure or delayed recovery of hair re-growth after shaving (arrows in Fig. 1C). When skin areas were analyzed by H&E staining, stained skin of wild-type mice revealed a typical architecture of the epidermal/dermal junction, with many hair follicles. In contrast, skins of mutant mice clearly showed an abnormal pattern of hair regeneration with shrinkage of the subcutaneous layer and a lower density of hair follicles in the epidermal layer (Fig. 1C and 1D).

To identify the cause of skin abnormalities in Brca1-S1152A mice, we used immunohistological analysis to study skin sections from aging-affected $Brca1^{S1152A/S1152A}$ animals in comparison with wild-type mice. In proliferating cells of wild-type mice, a Ki67-positive population was localized at the hair bulb region but such cells were distributed in many tiny follicles in $Brca1^{S1152A/S1152A}$ animals. To determine whether the Brca1-S1152A mutation corrupted skin architecture, we assessed skin sections using molecular markers of hair follicles (Fig. 2A). Thus, we examined expression of K6 and AE13, which are characteristic of keratinocytes of the outer root sheath and inner root sheath, respectively, in wild-type animals. In contrast, hair follicles of Brca1-S1152A mice displayed co-localization of K6 and AE13, unlike the separated wild-type phenotype. Interestingly, the hair follicle pattern in mutant mice was similar to that from 18 month-old animals in distribution and location of molecular markers including Ki67 and K6 (Fig. 2B). When the expression pattern of hair follicle markers in aged populations was compared, mutant animals displayed reduced expression of Ki67, K6, and AE13 compared with age-matched, wild-type mice. Together, these data indicate that the ATM-modifiable S1152 residue of Brca1 is required for proper skin structure formation and hair regeneration and that loss of ATM-regulation of Brca1-S1152 resulted in shortening of the lifespan with skin abnormalities characteristic of premature aging.

NIH-PA Author Manuscript

NIH-PA Author Manuscript

NIH-PA Author Manuscript

Delayed development and increased apoptosis in Brca1-S1152A mutant glands

Development of the mammary gland proceeds in distinct stages. Ductal elongation and branching occurs mainly during puberty, whereas alveolar proliferation and differentiation take place during pregnancy(28). Deletion of Brca1 from mammary epithelial cells resulted in aberrant mammary development (19). This finding prompted us to investigate whether Brca1-S1152A mutation caused phenotypical abnormalities in the development of the mammary gland.

To observe the ductal and alveolar development of the gland, we performed whole-mount staining of abdominal mammary glands of 2-month-old virgin female mice (Fig. 3A). We observed substantial alveolar development in wild-type animals (left panels of Fig. 3A). In contrast, the mammary gland of mutant mice was completely filled with a fat pad but displayed a delay in development with respect to duct and lobular formation. 22% (6/27) and 33% (9/27) of Brca1-S1152A mutant mice exhibited incomplete ductal development or lobular formation, respectively (right panels of Fig. 3A). H&E staining of mammary gland sections clearly showed the aberrant structure of the mutant gland compared with wild-type (Fig. 3B). However, despite the occurrence of mammary gland abnormalities in adolescent mutant mice, mutant animals showed the mature structure of mammary gland at 4 months of age (data not shown). It is because that the structure of normal mammary gland accomplishes within 2–3 month in virgin mice, and this structure remains the same unless mice become pregnant. Apparently, the Brca1-S1152A mutation delays, but does not blocks, the process of mammary gland development.

We have previously showed that pregnancy induced the hyperplastic changes in the mice lacking Brca1 in mammary gland (19). Thus, we also examined whether Brca1-S1152A mutant mice exhibited the mammary gland abnormalities in pregnancy, lactation, and involution periods. However, we could not find any differences between wild type and mutant mice in whole mount staining and histological analysis (data not shown). We also compared the capability of nursing the offspring and did not find a difference between $Brca1^{+/S1152A}$ and $Brca1^{S1152A/S1152A}$ mutant mice. The averaged offspring numbers of $Brca1^{+/S1152}$ (65 litters) and $Brca1^{S1152A/S1152A}$ (24 litters) at weaning time were 7.8 and 7.1 pups, respectively, without an obvious difference in body weight.

It has been reported that loss of Brca1 in the mammary gland causes increased apoptosis of epithelial cells and results in developmental abnormality with blunted ductal morphogenesis (19). To study mechanisms underlying the restricted development of the Brca1-S1152A mammary gland, we assessed cell proliferation and apoptosis in thoracic mammary glands of these mice (Fig. 3C and 3D). We observed similar levels of BrdU-positivity (26.8% *vs* 23.9%), but a statistically significant difference in apoptosis was apparent in Brca1-S1152A mutant mice (3.3%) compared with wild-type mice (0.19%). The results therefore indicate that signal communication between Brca1 and Atm is required for proper development of the mammary gland, in terms of regulation of apoptosis.

Brca1-S1152A mutant mice display hypersensitivity to γ-irradiation

Several lines of evidence indicate that a deficiency in BRCA1 causes a marked increase in DNA damage upon γ-irradiation (6). To determine whether the *Brca1*-S1152A mutation influenced sensitivity to γ-irradiation, we examined the levels of p53 protein in mouse embryonic fibroblasts (MEFs) derived from $Brca1^{S1152A/S1152A}$ and control embryos after 10 Gy irradiation. In wild-type MEFs, p53 levels began to increase from 1 h after irradiation and reached maximal levels by 4 h. However, in $Brca1^{S1152A/S1152A}$ MEFs, the level of p53 in untreated was rather high, but it did not increase after γ-irradiation (Fig. 4A). In addition, the level of p53 phosphorylated at Ser23 (p53-S23) rapidly increased in wild-type MEFs, by about 3.3-fold 1 h post-irradiation, and decreased substantially by 2 h. In contrast, the level of p53-

NIH-PA Author Manuscript

NIH-PA Author Manuscript

NIH-PA Author Manuscript

S23 peaked at 2 h (1.6-fold induction) and decreased notably by 4 h after treatment of *Brca1*-S1152A MEFs(Fig. 4A). We next investigated whether the *Brca1*-S1152A mutation modified cell cycle checkpoints in MEFs after γ-irradiation. However, we found that *Brca1*$^{S1152A/S1152A}$ MEFs showed no statistically significant defect in any of several cell cycle checkpoints analyzed, including the intra-S, G_2/M, and G_1/S checkpoints, after treatment with 10 Gy of irradiation (data not shown).

To further investigate the effect of Atm phosphorylation of Brca1 exon-11, we irradiated *Brca1*$^{S1152A/S1152A}$ mice and wild-type animals and compared their responses. Surprisingly, irradiation with 8 Gy markedly decreased the lifespan of *Brca1*-S1152A mutant mice (Mean=11.3 days) compared with wild-type animals (Mean=18.6 days) (Fig. 4B). No mutant *Brca1*$^{S1152A/S1152A}$ mice survived for longer than 14 days, whereas 7 of 14 (50%) wild-type animals lived beyond that time.

In an earlier study, animals carrying a null mutation in ATM displayed radiosensitivity of the intestine with extensive structural changes seen upon irradiation (29). Therefore, we were interested to determine whether *Brca1*-S1152A mice exhibited a similar phenotype. Thus, wild-type and *Brca1*$^{S1152A/S1152A}$ mice were irradiated with 8 Gy, followed by histological analysis of intestinal samples taken 3 days after irradiation. As shown in Fig. 4C, a marked shortening and rounding of villi was observed in *Brca1*-S1152A mutant mice but not in wild-type animals. The villus-to-crypt height ratios in the small intestine were 4±0.6 and 1.8±0.4 in wild-type and *Brca1*-S1152A mutant mice, respectively. Moreover, apoptotic signals in *Brca1*$^{S1152A/S1152A}$ mice were detected in a broad region of atrophic small intestinal mucosa, where as such signals were seldom seen in the mucosa of wild-type animals (Fig. 4D).

The results indicate that ATM and BRCA1 cooperate to prevent radiation-induced apoptosis and that BRCA1-S1189 is a key residue in this collaboration. Loss of this residue inhibits the DNA damage response induced by γ-irradiation.

Mammary gland hyperplasia and accelerated γ-irradiation-induced tumorigenesis in *Brca1*$^{S1152A/S1152A}$ mice

Our previous studies revealed that *Brca1*$^{\Delta 11/\Delta 11}$*Trp53*$^{+/-}$ mice showed normal mammary gland development and most of them developed mammary tumors within 6–10 months while none of *Trp53*$^{+/-}$ mice exhibited the neoplastic abnormalities in mammary gland in same period (17). However, *Brca1*$^{S1152A/S1152A}$ mice did not reveal any spontaneous mammary tumor formation (15 animals). However in six female *Brca1*$^{S1152A/S1152A}$ mice examined at 18 months of age, very dense branches were seen in mammary glands, with small hyperplasic foci, whereas no wild-type animal studied showed similar abnormalities at the same age (Fig. 5A). Pathological analysis of abnormal mammary glands from *Brca1*$^{S1152A/S1152A}$ mice displayed atypical hyperplasia (Fig. 5B). The S1152A-1 and S1152A-2 mutants showed lobular carcinomas *in situ* and atypical lobular hyperplasia. In the S1152A-3 mutant, we found the pathological findings described above and, additionally, an atypical microglandular adenosis. These abnormalities are not indicative of breast cancer but are accepted to be important markers for development of aggressive cancer (30).

To examine the molecular characteristics of hyperplastic mammary glands from *Brca1*-S1152A mice, we compared the expression levels of cyclin D1 and phosphorylated ER-α in sections from *Brca1*-S1152A mice with those in normal mammary glands of age-matched wild-type animals. As shown in Fig. 5C and 5D, mammary epithelial cells of *Brca1*$^{S1152A/S1152A}$ mice expressed greater levels of cyclin D1 and activation of ER-α than did wild-type animals. This indicates that the mutation in *Brca1*-S1152A increased expression of cyclin D1, and phosphorylation of ER-α, both of which are associated with increased cell proliferation.

NIH-PA Author Manuscript

NIH-PA Author Manuscript

NIH-PA Author Manuscript

Next, to determine the significance of ATM phosphorylation of the S1152 residue of BRCA1 in tumor prevention, we treated mice with a sublethal dose of γ-irradiation (3 Gy) four times at 1-week interval and studied the response. A significant tumorigenic alteration was induced by γ-irradiation of mutant mice, and this commenced at 3 months of age. Within the first year of life, 80% of mutant mice had developed tumors and all animals exhibited tumors by 18 months of age (Fig. 6A). In contrast, less than 20% (3 of 16) wild-type mice developed tumors during the same period. The main type of tumor was lymphoma in both mutant and wild-type animals. However, mutant mice showed a significantly higher frequency of tumor development than did wild-type animals. Four mutant mice developed mammary tumors, three developed liver tumors, and two exhibited tumors in two different organs (Fig. 6B). In addition to tumor formation, $Brca1^{S1152A/S1152A}$ mice showed hair graying after γ-irradiation (Fig. 6C). The cause and consequences of gray hair development in $Brca1^{S1152A/S1152A}$ mice after irradiation are not clear. However, gray hair development has also been reported in ATM- and Per2-deficient mice and in $Brca1^{S972A/S972A}$ animals, which also showed a high incidence of tumor formation (26,31,32).

Next, we performed an immunohistochemical analysis of mammary tumors from $Brca1^{S1152A/S1152A}$ mice to determine whether the pattern of molecular markers was similar to that of $Brca1^{\Delta 11/\Delta 11}$ mice (Fig. 6D). Differentiated adenocarcinomas from $Brca1^{S1152A/S1152A}$ mice were highly positive for cyclin D1, ER-α, and phospho-ER-α, but were negative for p53. Interestingly, neither ER-α nor phospho-ER-α was expressed in less-differentiated adenocarcinomas. These results are in agreement with our previous data illustrating a gradual reduction in ER-α expression with tumor progression in mammary tumors of $Brca1^{\Delta 11/\Delta 11}p53^{+/-}$ mice (33).

Together, these results show that ATM phosphorylation of the S1189 residue of BRCA1 is required for tumor prevention through modulation of p53 activity and apoptosis. Absence of this regulatory pathway leads to carcinogenesis.

DISCUSSION

The regulation of cellular responses to DNA damage is indispensable for maintenance of genomic stability. BRCA1 has a critical role in the early stages of this pathway through interacting with ATM, CHK2, and p53 (24,34,35). Our previous studies of Brca1 knockout mice have demonstrated the complicated mechanism by which BRCA1 protein affects genetic integrity. Comparisons between mutant and wild-type animals may provide clues to the understanding of BRCA1 biological functions. Null mutations in mouse *Brca1* led to embryonic lethality at E 6.5–8.5 (14–16). However, most $Brca1^{\Delta 11/\Delta 11}$ mice lacking the full-length protein but expressing the Δ11 isoform died at E 12.5–18.5, and a small proportion of mutant mice survived to adulthood but showed significant aging phenotypes (17,18). $Brca1^{\Delta 11/\Delta 11}$ mice could survive to adulthood in a mutated background for *p53*, *Chk2*, *p53BP1* or *ATM*, and all double mutant mice exhibited a high tumor incidence and phenotypes related to aging (18,35,36). $Brca1^{\Delta 11/\Delta 11}$ cells grew poorly and were defective in both the G_2/M cell cycle checkpoint and the spindle checkpoint (11,37). In contrast, $Brca1^{FL/FL}$ mice lacking the Δ11 isoform, but with the full-length protein, did not display any phenotype related to premature aging (20). Moreover, $Brca1^{FL/FL}$ cells grew normally and did not show any obvious defects in several major cell cycle checkpoints analyzed, indicating that exon-11 of BRCA1 may have an essential role in these processes.

During the DNA damage response, BRCA1 is extensively phosphorylated by several protein kinases, and this process is tightly linked to biological consequences (22). Thus, we tested whether impairment of regulation by phosphorylation of exon-11 of BRCA1 was responsible for the phenotypes characteristic of $Brca1^{\Delta 11\Delta 11}$. Previously, it had been reported that

NIH-PA Author Manuscript

NIH-PA Author Manuscript

NIH-PA Author Manuscript

phosphorylation by CHK2 of S988 of BRCA1, which is located in exon-11, was followed by a change in BRAC1 intracellular location (38). Thus, we generated and investigated a mouse model carrying the mutation S971A (S971 in mouse BRCA1 corresponds to S988 of human BRCA1) (26). We showed that *Brca1*$^{S971A/S971A}$ mice were at a moderately increased risk of spontaneous tumor formation, with a majority of females developing uterus hyperplasia and ovarian abnormalities by 2 years of age. Also, these mice exhibited acceleration of tumor formation after irradiation treatment. However, *Brca1*$^{S971A/S971A}$ animals did not display any developmental defect, irradiation sensitivity, or premature aging; these phenotypes were characteristic of *Brca1*- Δ11 mutant animals.

In the present report, we showed that *Brca1*-S1152A mutant and *Brca1*-Δ11 mutant mice shared phenotypes that were not found in *Brca1*-S971A mutant animals. First, *Brca1*$^{S1152A/S1152A}$ mice exhibited delayed development of mammary ducts and lobules, accompanied by an increased level of apoptosis, as also shown in conditional *Brca1* mutant mice, indicating that disruption of *Brca1* causes a developmental defect in the mammary gland by triggering apoptosis (19). Second, absence of the Brca1 full-length isoform causes senescence in mutant embryos and cultured cells, as well as aging and tumorigenesis in adult mice (18,35). The haploid loss of p53 or ATM overcame embryonic senescence but failed to prevent the adult mutant mice from aging prematurely, as shown by a decreased lifespan, reduced body fat deposition, osteoporosis, skin atrophy, and poor wound healing. Similarly, *Brca1*$^{S1152A/S1152A}$ mice displayed aging-like phenotypes including a shortened lifespan, reduced body weight, frequent skin damage, and lack of skin fat deposition. Next, we showed that the molecular markers of mammary tumors from *Brca1*-S1152A mutant mice exhibited a pattern similar to that from *Brca1*-Δ11 mutant animals. Cyclin D1 was detected in both types of mutant mice, in several stages of abnormal mammary gland development (39). ER-α signals were initially positive but became negative upon tumor progression, as also noted in the triple-negative tumors seen in BRCA1-deficient humans (33). Lastly, our previous report showed that *Brca1* mutant embryos exhibited a marked reduction in growth after γ-irradiation (16). Also, *Brca1*-S1152A mutant mice showed reduced survival, gut hypersensitivity, and increased tumor incidence after γ-irradiation. Although there are similarities in the phenotypes of *Brca1*-Δ11 and *Brca1*-S1152A mutant mice, abnormalities in animals carrying the *Brca1*-Δ11 mutation were much more severe than in mice with the *Brca1*-S1152A mutation. This is because exon-11 of BRCA1 comprises more than half the coding region, and interacts with several proteins including Rad50, Rad51, and Brca2 (40). Thus, loss of Brca1 exon-11 could logically result in development of more severe phenotypic characteristics than are associated with a single point mutation in an ATM phosphorylation site in this region. However, only *Brca1*-S1152A mutant mice showed similar phenotypes to those of *Brca1*-Δ11 mutant mice; *Brca1*-S971A and *Brca1*-FL mutant animals did not. Interestingly, *Brca1*$^{S1152A/S1152A}$ mice resembled ATM null-mutant animals, which also displayed premature aging, γ-irradiation hypersensitivity, and induction of tumorigenesis (29,31). Together, our data indicate that disruption of BRCA1 S1189 phosphorylation by ATM impairs the ability of BRCA1 and/or ATM to prevent tumor prevention and premature aging by inhibiting crosstalk between these two proteins.

In summary, BRCA1 is a large protein with multiple functional domains that interact with many proteins (40). In our continuous efforts to address the biological functions of BRCA1, we specifically mutated S1152 of mouse *Brca1*, which is uniquely phosphorylated by ATM in BRCA1 exon-11. Our data indicate that S1152 of BRCA1 has a specific role in longevity and that alteration of this amino acid results in development of aging-like phenotypes including growth retardation and skin abnormalities. Our data also show that alteration of S1152 in BRCA1 results in a change in the response to DNA damage, by affecting regulation of p53 activation and apoptosis. Although the influence of S1152-BRCA1 on tumor prevention is greater than in mice with a large deletion of the coding region, *Brca1*$^{S1152A/S1152A}$ mutant

NIH-PA Author Manuscript

NIH-PA Author Manuscript

NIH-PA Author Manuscript

animals exhibited atypical hyperplasia in the mammary gland over a long period. The mutant mice were also highly susceptible to tumorigenesis after γ-irradiation treatment, with increased tumor incidence and latency. These observations indicate that ATM-mediated phosphorylation of S1189 is required for BRCA1 in modulation of the DNA damage response and in repression of tumor formation.

Supplementary Material

Refer to Web version on PubMed Central for supplementary material.

Acknowledgments

This work was supported by the Intramural Research Program of the National Institute of Diabetes, Digestive, and Kidney Diseases, National Institutes of Health (Bethesda, MD) to C-XD, and the National Cancer Center of Korea (NCC-0910020), the Korea Healthcare Technology R & D Project (A090095), and the National Research Foundation of Korea (0930950) to SSK.

References

1. Sedgwick RP, Boder E. Progressive ataxia in childhood with particular reference to ataxia-telangiectasia. Neurology 1960;10:705–15. [PubMed: 14444443]
2. Lavin MF, Kozlov S. ATM activation and DNA damage response. Cell Cycle 2007;6:931–42. [PubMed: 17457059]
3. Abraham RT. Cell cycle checkpoint signaling through the ATM and ATR kinases. Genes & development 2001;15:2177–96. [PubMed: 11544175]
4. Alberg AJ, Helzlsouer KJ. Epidemiology, prevention, and early detection of breast cancer. Current opinion in oncology 1997;9:505–11. [PubMed: 9370070]
5. Brody LC, Biesecker BB. Breast cancer susceptibility genes. BRCA1 and BRCA2 Medicine 1998;77:208–26.
6. Deng CX. BRCA1: cell cycle checkpoint, genetic instability, DNA damage response and cancer evolution. Nucleic acids research 2006;34:1416–26. [PubMed: 16522651]
7. Lane TF, Deng C, Elson A, Lyu MS, Kozak CA, Leder P. Expression of Brca1 is associated with terminal differentiation of ectodermally and mesodermally derived tissues in mice. Genes & development 1995;9:2712–22. [PubMed: 7590247]
8. Miki Y, Swensen J, Shattuck-Eidens D, et al. A strong candidate for the breast and ovarian cancer susceptibility gene BRCA1. Science (New York, NY) 1994;266:66–71.
9. Thakur S, Zhang HB, Peng Y, et al. Localization of BRCA1 and a splice variant identifies the nuclear localization signal. Molecular and cellular biology 1997;17:444–52. [PubMed: 8972225]
10. Wilson CA, Payton MN, Elliott GS, et al. Differential subcellular localization, expression and biological toxicity of BRCA1 and the splice variant BRCA1-delta11b. Oncogene 1997;14:1–16. [PubMed: 9010228]
11. Xu X, Weaver Z, Linke SP, et al. Centrosome amplification and a defective G2-M cell cycle checkpoint induce genetic instability in BRCA1 exon 11 isoform-deficient cells. Molecular cell 1999;3:389–95. [PubMed: 10198641]
12. ElShamy WM, Livingston DM. Identification of BRCA1-IRIS, a BRCA1 locus product. Nat Cell Biol 2004;6:954–67. [PubMed: 15448696]
13. Deng CX, Xu X. Generation and analysis of Brca1 conditional knockout mice. Methods in molecular biology (Clifton, NJ) 2004;280:185–200.
14. Ludwig T, Chapman DL, Papaioannou VE, Efstratiadis A. Targeted mutations of breast cancer susceptibility gene homologs in mice: lethal phenotypes of Brca1, Brca2, Brca1/Brca2, Brca1/p53, and Brca2/p53 nullizygous embryos. Genes & development 1997;11:1226–41. [PubMed: 9171368]
15. Liu CY, Flesken-Nikitin A, Li S, Zeng Y, Lee WH. Inactivation of the mouse Brca1 gene leads to failure in the morphogenesis of the egg cylinder in early postimplantation development. Genes & development 1996;10:1835–43. [PubMed: 8698242]

NIH-PA Author Manuscript

NIH-PA Author Manuscript

NIH-PA Author Manuscript

16. Shen SX, Weaver Z, Xu X, et al. A targeted disruption of the murine Brca1 gene causes gamma-irradiation hypersensitivity and genetic instability. Oncogene 1998;17:3115–24. [PubMed: 9872327]
17. Xu X, Qiao W, Linke SP, et al. Genetic interactions between tumor suppressors Brca1 and p53 in apoptosis, cell cycle and tumorigenesis. Nature genetics 2001;28:266–71. [PubMed: 11431698]
18. Cao L, Li W, Kim S, Brodie SG, Deng CX. Senescence, aging, and malignant transformation mediated by p53 in mice lacking the Brca1 full-length isoform. Genes & development 2003;17:201–13. [PubMed: 12533509]
19. Xu X, Wagner KU, Larson D, et al. Conditional mutation of Brca1 in mammary epithelial cells results in blunted ductal morphogenesis and tumour formation. Nature genetics 1999;22:37–43. [PubMed: 10319859]
20. Kim SS, Cao L, Lim SC, et al. Hyperplasia and spontaneous tumor development in the gynecologic system in mice lacking the BRCA1-Delta11 isoform. Molecular and cellular biology 2006;26:6983–92. [PubMed: 16943438]
21. Yoshida K, Miki Y. Role of BRCA1 and BRCA2 as regulators of DNA repair, transcription, and cell cycle in response to DNA damage. Cancer Sci 2004;95:866–71. [PubMed: 15546503]
22. Ouchi T. BRCA1 phosphorylation: biological consequences. Cancer Biol Ther 2006;5:470–5. [PubMed: 16721040]
23. Lavin MF, Birrell G, Chen P, Kozlov S, Scott S, Gueven N. ATM signaling and genomic stability in response to DNA damage. Mutat Res 2005;569:123–32. [PubMed: 15603757]
24. Cortez D, Wang Y, Qin J, Elledge SJ. Requirement of ATM-dependent phosphorylation of brca1 in the DNA damage response to double-strand breaks. Science (New York, NY) 1999;286:1162–6.
25. Wang Y, Cortez D, Yazdi P, Neff N, Elledge SJ, Qin J. BASC, a super complex of BRCA1-associated proteins involved in the recognition and repair of aberrant DNA structures. Genes & development 2000;14:927–39. [PubMed: 10783165]
26. Kim SS, Cao L, Li C, et al. Uterus hyperplasia and increased carcinogen-induced tumorigenesis in mice carrying a targeted mutation of the Chk2 phosphorylation site in Brca1. Molecular and cellular biology 2004;24:9498–507. [PubMed: 15485917]
27. Lakso M, Pichel JG, Gorman JR, et al. Efficient in vivo manipulation of mouse genomic sequences at the zygote stage. Proceedings of the National Academy of Sciences of the United States of America 1996;93:5860–5. [PubMed: 8650183]
28. Hennighausen L, Robinson GW. Think globally, act locally: the making of a mouse mammary gland. Genes & development 1998;12:449–55. [PubMed: 9472013]
29. Elson A, Wang Y, Daugherty CJ, et al. Pleiotropic defects in ataxia-telangiectasia protein-deficient mice. Proceedings of the National Academy of Sciences of the United States of America 1996;93:13084–9. [PubMed: 8917548]
30. Dupont WD, Parl FF, Hartmann WH, et al. Breast cancer risk associated with proliferative breast disease and atypical hyperplasia. Cancer 1993;71:1258–65. [PubMed: 8435803]
31. Barlow C, Eckhaus MA, Schaffer AA, Wynshaw-Boris A. Atm haploinsufficiency results in increased sensitivity to sublethal doses of ionizing radiation in mice. Nature genetics 1999;21:359–60. [PubMed: 10192382]
32. Fu L, Pelicano H, Liu J, Huang P, Lee C. The circadian gene Period2 plays an important role in tumor suppression and DNA damage response in vivo. Cell 2002;111:41–50. [PubMed: 12372299]
33. Li W, Xiao C, Vonderhaar BK, Deng CX. A role of estrogen/ERalpha signaling in BRCA1-associated tissue-specific tumor formation. Oncogene 2007;26:7204–12. [PubMed: 17496925]
34. Gatei M, Scott SP, Filippovitch I, et al. Role for ATM in DNA damage-induced phosphorylation of BRCA1. Cancer Res 2000;60:3299–304. [PubMed: 10866324]
35. Cao L, Kim S, Xiao C, et al. ATM-Chk2-p53 activation prevents tumorigenesis at an expense of organ homeostasis upon Brca1 deficiency. EMBO J 2006;25:2167–77. [PubMed: 16675955]
36. Cao L, Xu X, Bunting SF, et al. A selective requirement for 53BP1 in the biological response to genomic instability. Molecular cell. in press.
37. Wang RH, Yu H, Deng CX. A requirement for breast-cancer-associated gene 1 (BRCA1) in the spindle checkpoint. Proceedings of the National Academy of Sciences of the United States of America 2004;101:17108–13. [PubMed: 15563594]

NIH-PA Author Manuscript

NIH-PA Author Manuscript

NIH-PA Author Manuscript

38. Lee JS, Collins KM, Brown AL, Lee CH, Chung JH. hCds1-mediated phosphorylation of BRCA1 regulates the DNA damage response. Nature 2000;404:201–4. [PubMed: 10724175]

39. Brodie SG, Xu X, Qiao W, Li WM, Cao L, Deng CX. Multiple genetic changes are associated with mammary tumorigenesis in Brca1 conditional knockout mice. Oncogene 2001;20:7514–23. [PubMed: 11709723]

40. Deng CX, Brodie SG. Roles of BRCA1 and its interacting proteins. Bioessays 2000;22:728–37. [PubMed: 10918303]

NIH-PA Author Manuscript
NIH-PA Author Manuscript
NIH-PA Author Manuscript

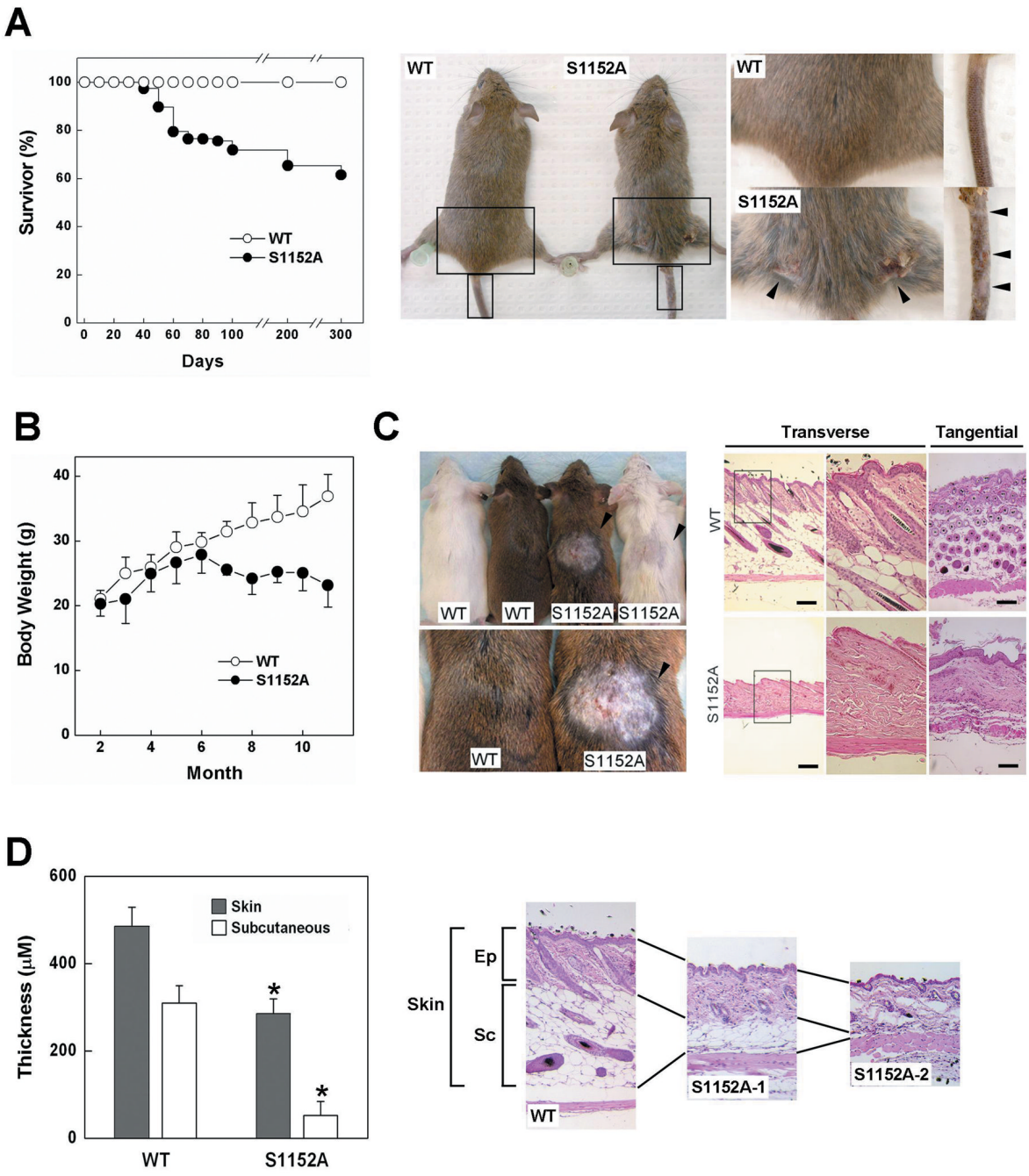

Fig. 1. Aging-like phenotypes of *Brca1*$^{S1152A/S1152A}$ mice

(A) Lifespan and skin abnormalities of *Brca1*$^{S1152A/S1152A}$ mice. Representing photography of skin damage in aging-affected *Brca1*$^{S1152A/S1152A}$ animal is shown with wild type mouse. Arrows indicate the area of wounds. The boxed areas are magnified on the right. (B) *Brca1*$^{S1152A/S1152A}$ female mice weighed significantly less than their wild-type littermates between 7 and 11 months of age (n=10, P<0.01). (C) Pattern of hair re-growth and H&E staining of skin sections 1 week after shaving and wounding. Transverse (1st and 2nd panels) and tangential (3rd panels) sections of skins are shown in right side. (D) Quantitative measurement of skin and hypodermis thickness. Skin tissues were collected in the center of back skin from wild type (N=8) and *brca1*$^{S1151A/S1152A}$ mutant (N=7) mice. After histological process, the

thicknesses of skins were measured in 3 different locations in each section under the microscope. Statistically significant differences ($P<0.01$) are indicated by asterisks. Bars, 200 μm. Ep, epidermis; Sc, subcutaneous; WT, wild-type; S1152A, *Brca1*$^{S1152A/S1152A}$.

NIH-PA Author Manuscript
NIH-PA Author Manuscript
NIH-PA Author Manuscript

NIH-PA Author Manuscript
NIH-PA Author Manuscript
NIH-PA Author Manuscript

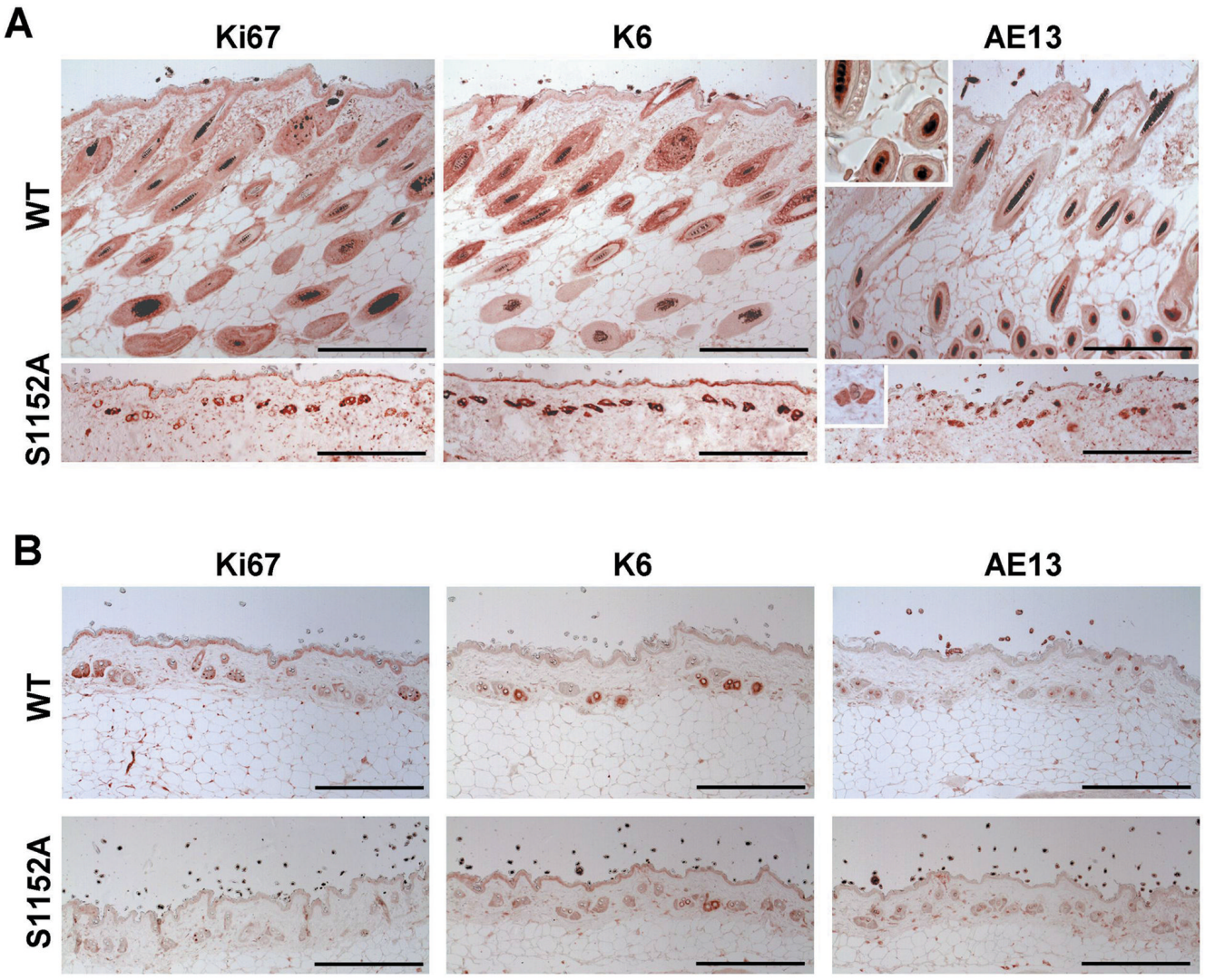

Fig. 2. Immunohistochemical analysis of *Brca1*$^{S1152A/S1152A}$ mice skin

Immunohistochemical staining of skin sections were performed on wild-type and aging-affected *Brca1*$^{S1152A/S1152A}$ mice (A) and 18 months (B) of age. Sections were imaged using primary antibodies against Ki67, K6, and AE13. Bars, 200 μm. WT, wild-type; S1152A, *Brca1*$^{S1152A/S1152A}$.

NIH-PA Author Manuscript

NIH-PA Author Manuscript

NIH-PA Author Manuscript

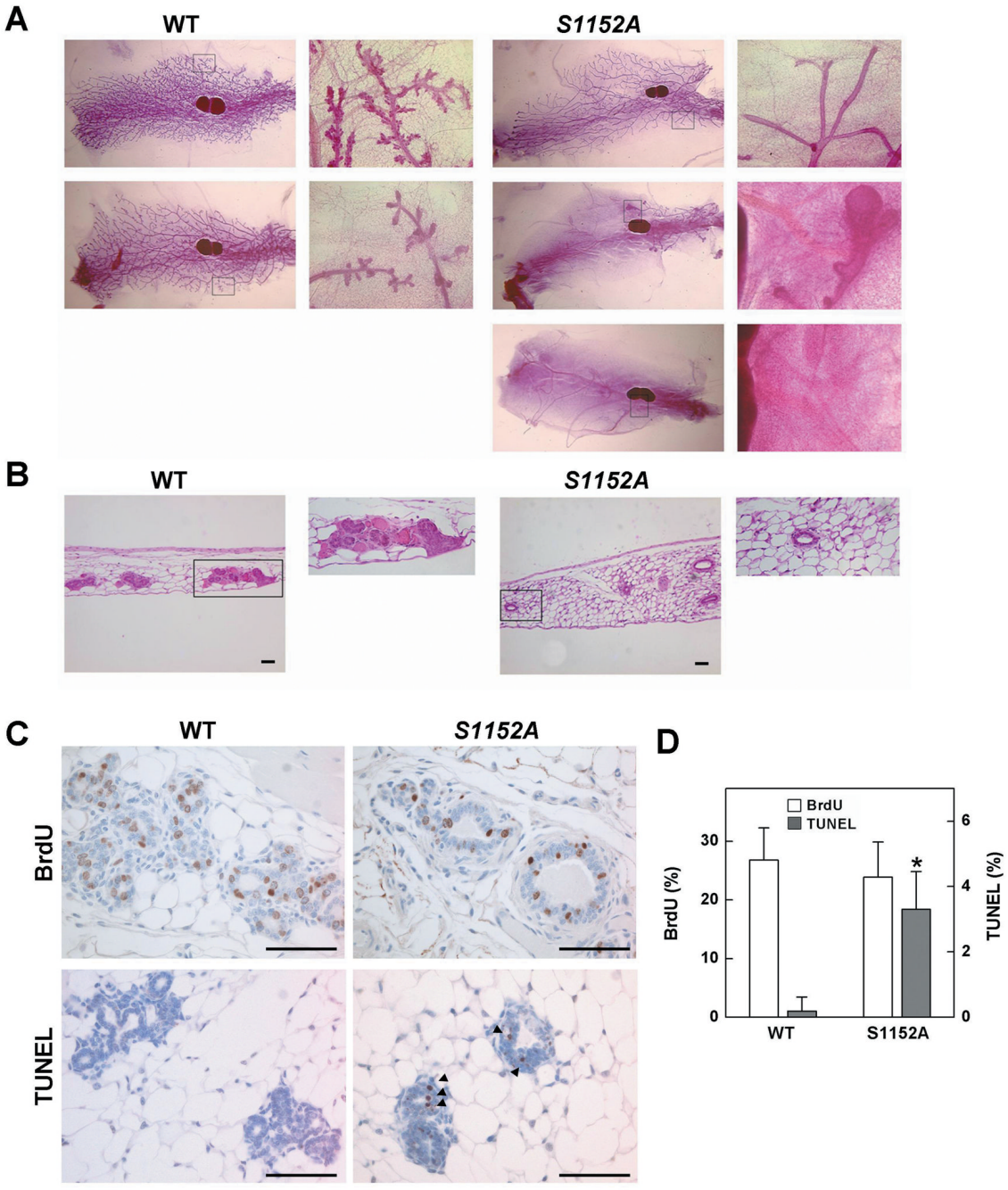

Fig. 3. Delayed development of the mammary gland of *Brca1*$^{S1152A/S1152A}$ mice

Whole mount (A) and H&E (B) staining of abdominal mammary glands from 2-month-old *Brca1*$^{S1152A/S1152A}$ and age-matched wild-type (WT) female mice. The right panels indicate amplification of boxed areas. (C) Immunohistochemical staining of 2-month-old mammary gland sections from *Brca1*$^{S1152A/S1152A}$ and WT mice. Sections were imaged using a primary antibody against BrdU and TUNEL staining. Arrows indicate TUNEL-positive cells. (D) Quantification of BrdU- and TUNEL-positive cells. After staining of mammary glands from wild type (N=12) and *Brca1*$^{S1151A/S1152A}$ mutant (N=11) mice, at least 100 epithelial cells were counted in each staining for calculation of BrdU incorporation and TUNEL positive rates.

NIH-PA Author Manuscript

NIH-PA Author Manuscript

NIH-PA Author Manuscript

Statistically significant differences ($P<0.01$) are indicated by asterisks. Bars, 100 μm. WT, wild-type; S1152A, *Brca1*$^{S1152A/S1152A}$.

NIH-PA Author Manuscript

NIH-PA Author Manuscript

NIH-PA Author Manuscript

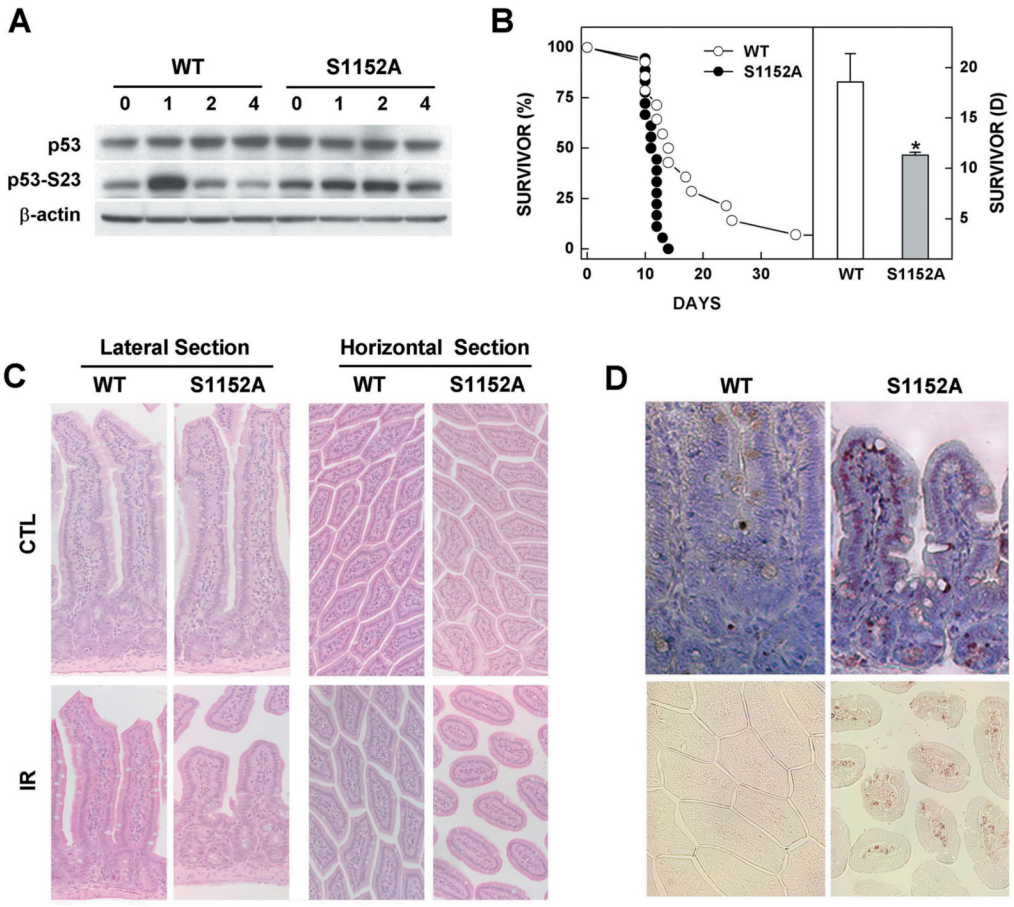

Fig. 4. Phenotypes of the *Brca1*$^{S1152A/S1152A}$ mutant in response to γ-irradiation

(A) Protein expression patterns in MEFs from wild-type and *Brca1*$^{S1152A/S1152A}$ embryos after 10 Gy irradiation. (B) Kaplan-Meier survival curve of 4-weeks-old *Brca1*$^{S1152A/S1152A}$ (n=18) mice and wild-type littermates (n=14) after exposure to 8 Gy of irradiation. Statistically significant differences (P<0.01) are indicated by asterisks. (C) Lateral and horizontal sections of small intestines from 8 Gy-irradiated wild-type and *Brca1*-S1152A mutant mice. (D) Apoptotic cells detected by TUNEL staining are shown in lateral and horizontal views in the upper and lower panels, respectively. WT, wild-type; S1152A, *Brca1*$^{S1152A/S1152A}$.

NIH-PA Author Manuscript

NIH-PA Author Manuscript

NIH-PA Author Manuscript

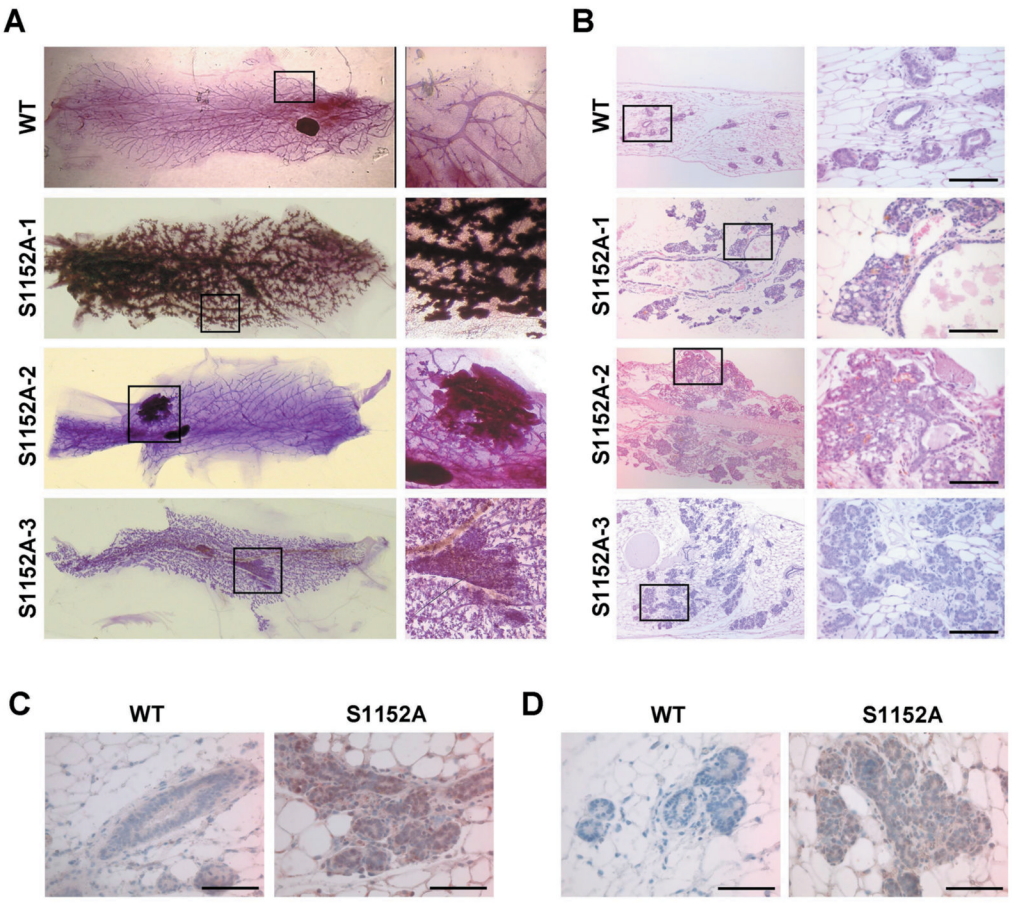

Fig. 5. Mammary gland abnormalities in *Brca1*$^{S1152A/S1152A}$ mice

Whole-mount (A), H&E (B), and immunohistochemical (C, D) staining of mammary glands from *Brca1*$^{S1152A/S1152A}$ and wild-type mice at 18 months of age. The boxed areas are amplified and displayed on the right. Immunohistochemical imaging was achieved using primary antibodies against cyclin D1 (C) and phospho-ER-α (D). Bars, 100 μm. WT, wild-type; S1152A, *Brca1*$^{S1152A/S1152A}$.

NIH-PA Author Manuscript

NIH-PA Author Manuscript

NIH-PA Author Manuscript

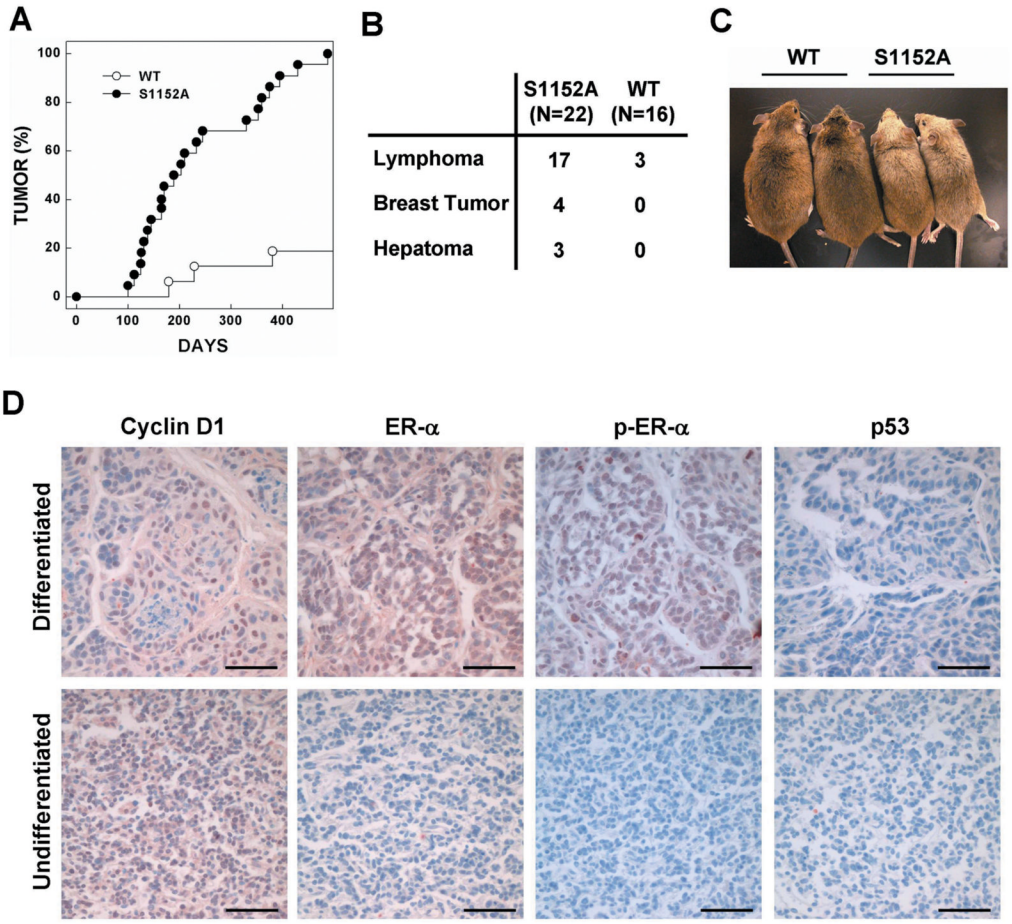

Fig. 6. Reduced survival and a high tumor incidence in *Brca1*$^{S1152A/S1152A}$ mice treated with γ-irradiation

(**A**) Kaplan-Meier survival curve of wild-type (WT, n=22) and *Brca1*$^{S1152A/S1152A}$ (S1152A, n=16) mice after irradiation. (B) Tumor spectrum of mice after irradiation. Two mutant mice had tumors in more than one organ. (C) Wild-type (WT) and *Brca1*$^{S1152A/S1152A}$ (S1152A) mice at 10 months after irradiation. (D) Immunohistochemical staining of mammary tumor sections from *Brca1*$^{S1152A/S1152A}$ and WT mice. Images of sections were detected using primary antibodies against cyclin D1, ER-α, phospho-ER-α, and p53. Bars, 50 μm.